Preprints.org

Communication

Not peer-reviewed version

Combined Displacement and Angle Sensor with Ultrahigh Compactness Based on Self-imaging Effect of Optical Microgratings

Mengdi Zhang , Hao Yang , Qianqi Niu , Xuye Zhang , Jiaan Yang , Jiangbei Lai , Changjiang Fan , Mengwei Li * , Chenguang Xin *

Posted Date: 27 December 2023

doi: 10.20944/preprints202312.2100.v1

Keywords: self-imaging effect; optical micrograting; combined sensor; multi degree of freedom; displacement

Preprints.org is a free multidiscipline platform providing preprint service that is dedicated to making early versions of research outputs permanently available and citable. Preprints posted at Preprints.org appear in Web of Science, Crossref, Google Scholar, Scilit, Europe PMC.

Copyright: This is an open access article distributed under the Creative Commons Attribution License which permits unrestricted use, distribution, and reproduction in any medium, provided the original work is properly cited.

Preprints (www.preprints.org) | NOT PEER-REVIEWED | Posted: 27 December 2023 doi:10.20944/preprints202312.2100.v1

Disclaimer/Publisher's Note: The statements, opinions, and data contained in all publications are solely those of the individual author(s) and contributor(s) and not of MDPI and/or the editor(s). MDPI and/or the editor(s) disclaim responsibility for any injury to people or property resulting from any ideas, methods, instructions, or products referred to in the content.

Communication

Combined Displacement and Angle Sensor with Ultrahigh Compactness Based on Self-Imaging Effect of Optical Microgratings

Mengdi Zhang [1], Hao Yang [1], Qianqi Niu [1], Xuye Zhang [1], Jiaan Yang [1], Jiangbei Lai [1], Changjiang Fan [1], Mengwei Li [1,2,*] and Chenguang Xin [1,2,*]

[1] School of Instrument and Electronics, North University of China, Taiyuan 030051, China
[2] School of Instrument and Intelligent Future Technology, North University of China, Taiyuan 030051, China
* Correspondence: lmw@nuc.edu.cn, Tel.: +86-13934248366; xincg@nuc.edu.cn, Tel.: +86-17836211946

Abstract: In this paper, an ultracompact combined sensor for displacement and angle synchronous measurement is proposed based on self-imaging effect of optical microgratings. Using a two-grating structure, linear and angular displacement can be measured by detecting the change of phase and amplitude of the optical transmission respectively within one single structure in meantime. The optical transmitted properties of the two-grating structure are investigated in both theory and simulation. Simulated results indicate that, the optical transmission changes in a sinusoidal relationship to the input linear displacement. Meanwhile, the amplitude of the curve decreases with an input pitch angle, indicating the ability for synchronous measurement within one single compact structure. The synchronous measurement of the linear displacement and the angle is also demonstrated experimentally. The results show a resolution down to 4nm for linear displacement measurement, and a sensitivity of 0.26mV/arcsec within a range of ±1° for angle measurement. Benefitting from a simple common-path structure without using optical components including reflectors and polarizers, the sensor shows an ultrahigh compactness for multiple-degrees-of-freedom measuring, indicating the great potential for this sensor in the fields such as integrated mechanical positioning and semiconductor fabrication.

Keywords: self-imaging effect; optical micrograting; combined sensor; multi degree of freedom; displacement

1. Introduction

Precision measurement with multiple degrees of freedom (DOF) can be used to accurately detect the position and presence of objects in planar or three-dimensional space, which have been widely used in machining positioning and motion driving in ultra-precision machining processes [1–3]. The measured degrees of freedom typically include linear parameters (e.g., displacement in three linear axes) and angular parameters (e.g., roll angle, yaw angle and pitch angle) [4,5]. In past decades, several optical methods have been reported for multiple-DOF measurement, including laser interferometry, autocollimation and grating diffraction interferometry [6–8]. Among these methods, the grating-based approach shows high resolution and stability for compact machining systems [9,10]. Generally, multiple-DOF measurement based on optical gratings can be demonstrated by either using multiple linear displacement sensors or combining the optical interference and the autocollimation [11–13]. Considering the recent compelling need for developing ultracompact components for high-precision machining systems such as lithography machines [14]. In 2013, X. Li *et al.* present a multi-axis surface encoder to measure 6-DOF translational displacement motions and angular motions of a planar motion stage. The measurement resolutions of the displacement and angle are about 1nm and 0.1'' [15]. In 2022, S. Wang *et al.* proposed a grating encoder which can provide absolute 4-DOF position and pose monitoring with sub-arcsecond and sub-micron accuracy

© 2023 by the author(s). Distributed under a Creative Commons CC BY license.

[16]. In the case, plenty of optical components including reflectors, polarizers, wave plates are required for synchronously measuring the linear and the angular parameters, resulting in a low compactness and significant degradation of accuracy caused by large Abbe error and cross-talk error [17,18].

The self-imaging effect reveals a phenomenon that, when a periodic structure (e.g., optical grating) is irradiated by a plane wave, the intensity distribution of the optical field at certain distances behind the structure shows a same period [19]. Benefitting from a simple optical path and high compactness, either linear or angular measurement has been demonstrated in past years based on the self-imaging effect of optical gratings. For linear displacement measurement, in 2014, P. Rodriguez-Montero *et al.* present a device for measuring displacement based on the self-imaging and the nonsteady photo-electromotive force effects, demonstrating an estimated resolution better than 10μm within a dynamic range of 1.5mm [20]. In 2015, S. Agarwal *et al.* reported an in-plane displacement measurement by using a circular grating Talbot interferometer [21]. By analyzing the shift of self-imaging interferometric fringe patterns, a resolution at micrometer level was reported. In 2022, C. Xin *et al.* improved the resolution to be 0.73nm within a range up to mm level by using a two-quadrant detector [22]. For angular measurement, in 1999, Q. Liu *et al.* found the Moire fringes changing with different parallelism between two optical gratings [23]. In 2006, A. Wang *et al.* reported a sensor that used the self-imaging effect to detect the local intensity and incident angle of light [24]. In 2022, Z. Yang *et al.* reported an ultracompact angular displacement sensor using a double-grating structure with a sensitivity of 0.19mV/arcsec within a range of ± 396arcsec [25]. Since both the linear and angular displacement synchronously changing the amplitude of the output signal or the patterns of the self-imaging images in the cases mentioned above, the linear and angular displacement is hard to be distinguished from each other. By using different parameters (e.g., amplitude and phase respectively) of the output signals, the self-imaging effect can be in principle used in developing multiple-DOF measuring with high compactness and accuracy.

In this paper, an ultra-compact composite displacement and angle sensor based on the self-imaging effect of optical microgratings is demonstrated. By detecting the change in the phase and the amplitude of optical transmission behind two gratings, the linear displacement and angle can be measured synchronously. The simulated results obtained by a finite-difference time-domain (FDTD) method show that, the transmission changes sinusoidally with a relative linear displacement between two gratings. The phase of the sinusoidal signal is related to the input linear displacement (e.g., a phase of 2π corresponding to a linear displacement equal to one single period of the grating). And the amplitude of the sinusoidal signal attenuates with an increasing pitch angle for the upper grating. A resolution of 4nm for linear displacement and 3.85arcsec within a range of ±1° for angle measurement have been demonstrated experimentally, indicating the ability for synchronous multiple-DOF measurement. Benefitting from a simple coaxial optical path without using much optical components such as reflectors and polarizers, this sensor shows ultrahigh compactness for multi-DOF measurement without significant degradation of accuracy compared to traditional one-dimension measurement [22], showing the great potential in applications ranging from integrable high-precision machining to manufacturing.

2. Principle

The measuring principle of the proposed sensor can be explained by a plane wave interference theory. A double-layer structure consisting of two optical microgratings with a same period is used. When a monochromatic plane wave is vertically incident on an optical grating, the amplitude transmission behind the grating can be expressed as [26]

$$t(x) = \sum_{n=-\infty}^{\infty} C_n \exp\left(i2\pi \frac{n}{d} x\right) \tag{1}$$

where C_n is the Fourier coefficient and d is the grating period.

Assuming that the lower grating (G2) is located behind the upper grating (G1) with a certain distance of NZ_T, (N=0,1,2...), where

Preprints (www.preprints.org) | NOT PEER-REVIEWED | Posted: 27 December 2023 doi:10.20944/preprints202312.2100.v1

$$Z_T = \frac{2d^2}{\lambda} \tag{2}$$

is the period of the self-imaging images in the direction perpendicular to the plane of grating [27].

Assuming that G1 rotates along the y axis with an angle of θ synchronously, the two gratings were no longer parallel to each other. Using a projective simplification, G1 can be projected into a parallel plane after being rotated. In this case, the modified grating period (d) can be given by $d\cos\theta$, and self-imaging positions is defined by $Z=Z_T'=2d^2\cos^2\theta/\lambda$.

Assuming that the distance between G1 and G2 is Z, the complex amplitude distribution of the light field at lower surface of G2 can be expressed as

$$U(x,z) = \exp(ikz)\sum_{n=-\infty}^{\infty} C_n \exp\left(i2\pi \frac{n}{d\cos\theta}x\right) \tag{3}$$

Assuming that G1 and G2 have a relative displacement, the complex amplitude distribution behind G2 can be given [25]

$$U'(x,z,\Delta L) = \exp(ikz)\sum_{n=-\infty}^{\infty}\sum_{m=-\infty}^{\infty} C_n C_m \exp\left[i2\pi \frac{(n/\cos\theta)+m}{d}x\right]\exp\left[i2\pi \frac{n/\cos\theta}{d}\Delta L\right] \tag{4}$$

where ΔL is the relative linear displacement between G1 and G2.

The Eq. (4) indicates that, $U'(x,z,\Delta L)$ changes sinusoidally with an input linear displacement. Since the system can be regarded as a low-pass filter in which the components whose spatial frequency is higher than that of the gratings are cut off, the phase of the sinusoidally curve is related to the displacement by a factor of $1/d\cos\theta$, which means that each change of 2π in phase corresponding to a linear displacement of $d\cos\theta$ [23]. Meanwhile, the amplitude of the curve is related to the input angle with a factor of $1/\cos\theta$. As a result, it is possible in principle to measure the linear and angular displacement at same time by detecting the phase and the amplitude respectively.

3. Simulation

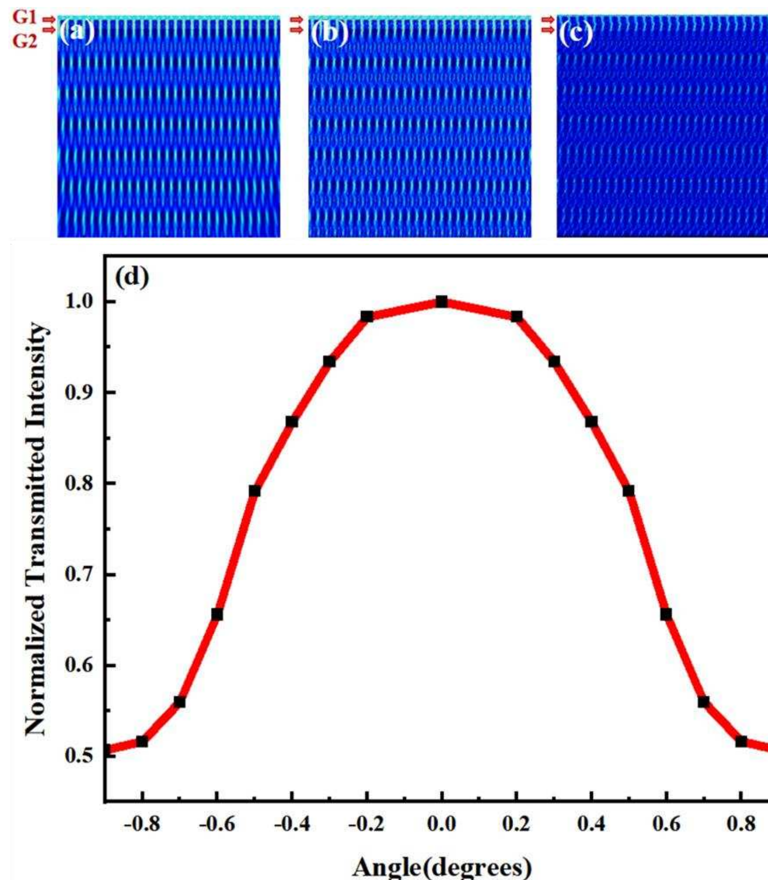

Figure 1. Simulated optical transmission behind two optical gratings with **(a)** θ=0°, **(b)** θ=1° and **(c)** θ=2°. The positions of the two gratings are indicated by the red arrows. The period of the gratings used in the simulation is of 4μm. **(d)** Simulated transmitted intensity with different θ.

The optical transmitted properties of a double-grating structure are investigated by a FDTD method. The material of the gratings is aluminum. The period of the gratings is of 4μm. And the wavelength of the input beam is 635nm. The simulated optical transmission with different θ is shown in Figure 1(a)(b)(c). As θ increasing from 0° to 2° gradually, the transmission decreases meanwhile, agreeing with theoretical analysis. The normalized simulated transmitted intensity with different θ is shown in Figure 1(d). A maximum normalized intensity of 1 is obtained as θ=0°. As $|\theta|$ increases, the normalized intensity decreases as well (e.g., down to 0.51 as $|\theta|$=0.9°).

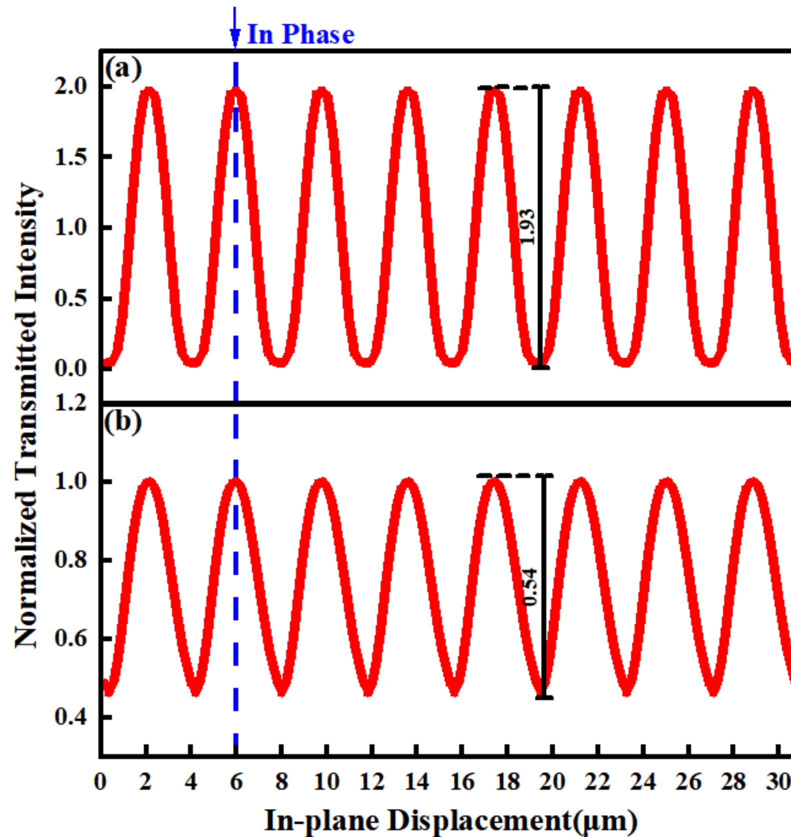

Figure 2. The transmitted intensity with different θ of 0° and 1° respectively as there is an input linear displacement.

The transmitted intensity with different θ of 0° and 1° respectively as there is an input linear displacement is shown in Figure 2. With a relative linear displacement between G1 and G2 along the in-plane direction perpendicular to the grating lines, the transmitted intensity changes sinusoidally with the input displacement in both cases. However, the change of θ results in a different amplitude. The amplitude of the sinusoidal signal decreases from 1.93 to 0.54 as θ changing from 0° to 1°. It is worth to mention that, despite the different amplitudes, the sinusoidal signals in the two cases approximatively remains in a same phase with a small rotated angle, which means that the input linear displacement and angle can be distinguished by the phase and amplitude respectively.

4. Experimental

4.1. Self-imaging effect of one single optical grating

Preprints (www.preprints.org) | NOT PEER-REVIEWED | Posted: 27 December 2023 doi:10.20944/preprints202312.2100.v1

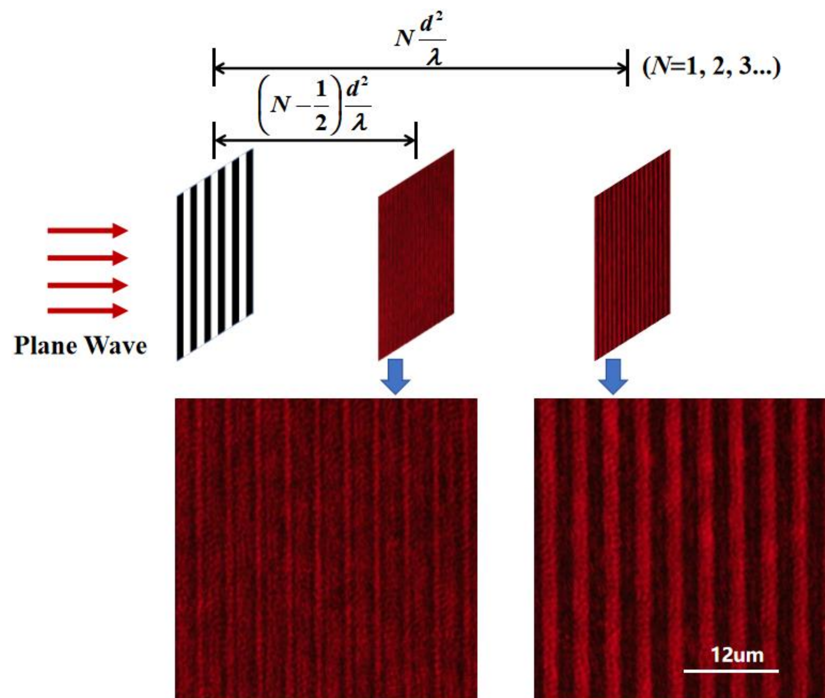

Figure 3. The self-imaging patterns behind a 4μm-period grating at different positions obtained experimentally.

The self-imaging patterns behind a 4μm-period grating is shown in Figure 3. The wavelength of the input plane wave is 635nm. A microscope system consisted of a 40× object lens and a CCD (M830, Murzider) is located behind the grating. As microscope system moving along the optical axis, the self-imaging patterns as different locations behind the grating can be obtained. Subdivided patterns and self-imaging patterns with period of 2μm and 4μm are obtained at positions of $(N\text{-}½)d^2/\lambda$ and Nd^2/λ (N=1,2,3...) respectively, agreeing with the theoretical analysis of the self-imaging effects [28].

4.2. Combined displacement and angle measurement with double gratings

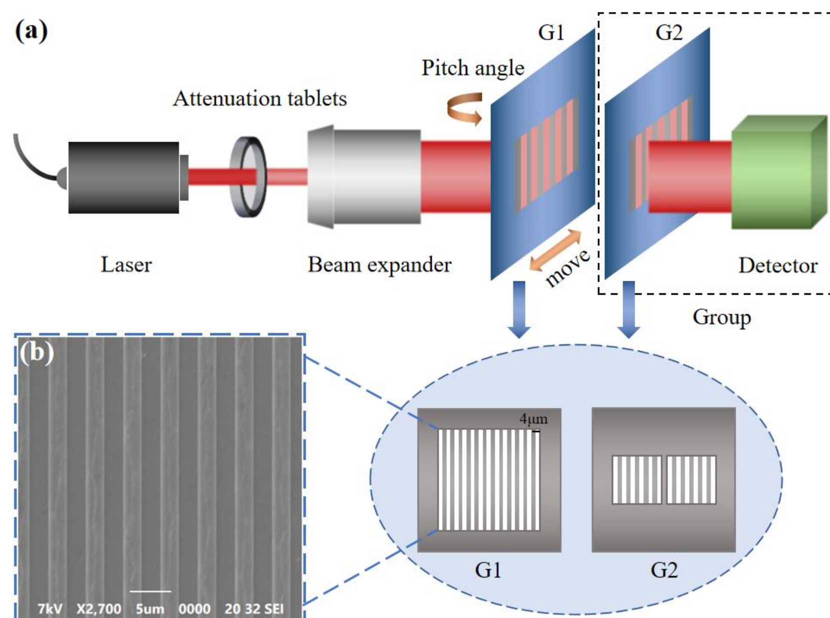

Preprints (www.preprints.org) | NOT PEER-REVIEWED | Posted: 27 December 2023 doi:10.20944/preprints202312.2100.v1

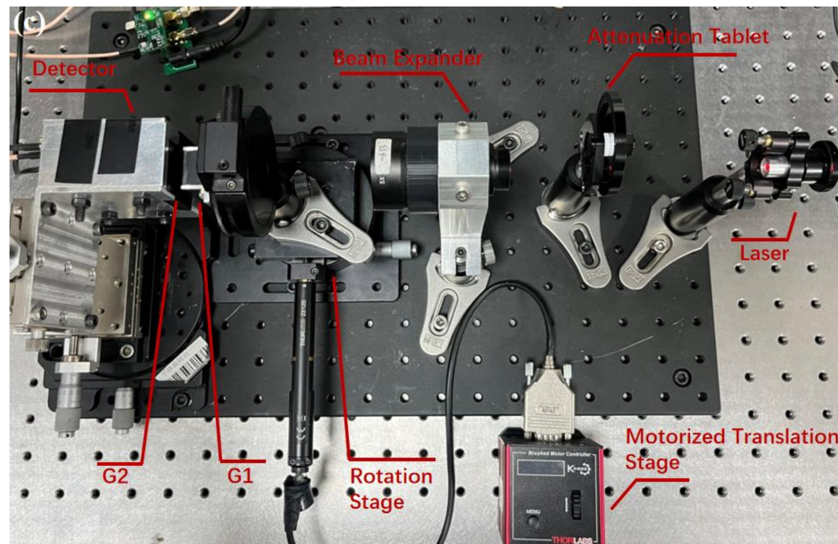

Figure 4. (a) Schematic diagram of the combined displacement and angle sensor. **(b)** Scanning electron microscope image of G1 used in the experiment. **(c)** Optical image of the experimental setup.

The schematic diagram of the experiment is shown in Figure 4. The beam with a wavelength of 635nm from the laser (CPS635R, Thorlabs) irradiate onto two gratings. G2 is fabricated in a two-quadrant structure to obtain two sinusoidal signals with a phase difference of 90° [22]. The gratings are prepared by etching aluminum film with a thickness of 150nm, which is located on a silicon dioxide substrate with a thickness of 500μm. The structure of the grating and the image under electron microscope are shown in Figure 4(b), scanning electron microscopy image demonstrates a grating period of 4μm and duty ratio is 0.5. A multi-quadrant detector (OSQ100-IC, OTRON) is placed behind G2 to measure the transmitted intensity.

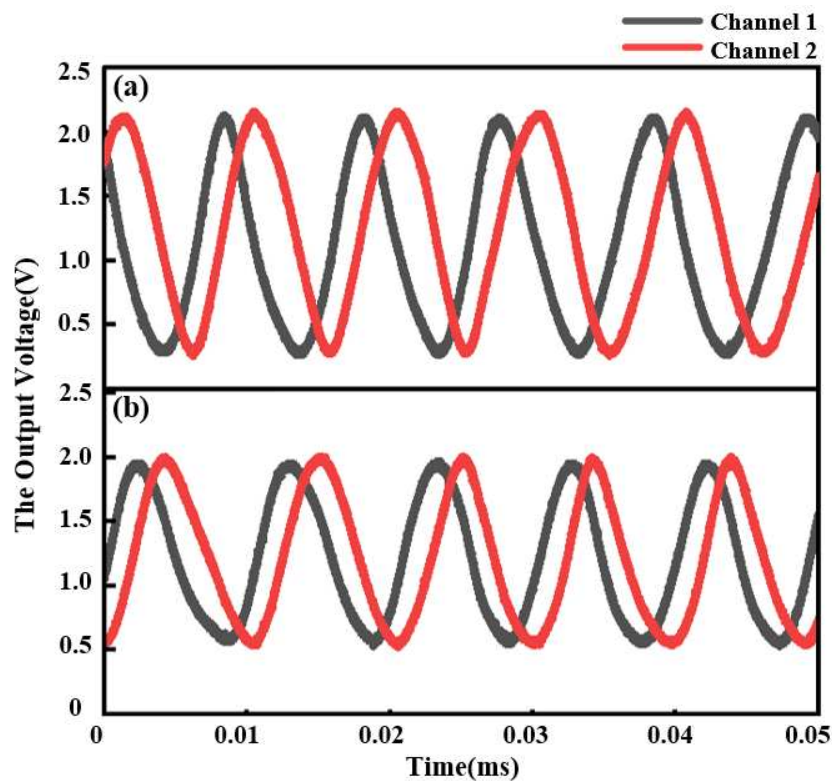

Figure 5. Experimental results with different θ of **(a)** 0° and **(b)** 1° respectively with a uniform-rate input linear displacement.

Preprints (www.preprints.org) | NOT PEER-REVIEWED | Posted: 27 December 2023 doi:10.20944/preprints202312.2100.v1

The sinusoidal signals obtained from the multi-quadrant detector with different θ is shown in Figure 5. Corresponding to the simulated results mentioned above, the amplitude of the output signals decreases from 1.88V to 1.4V as θ changing from 0° to 1°. And with a uniform-rate input linear displacement, the phase of the signals changes meanwhile.

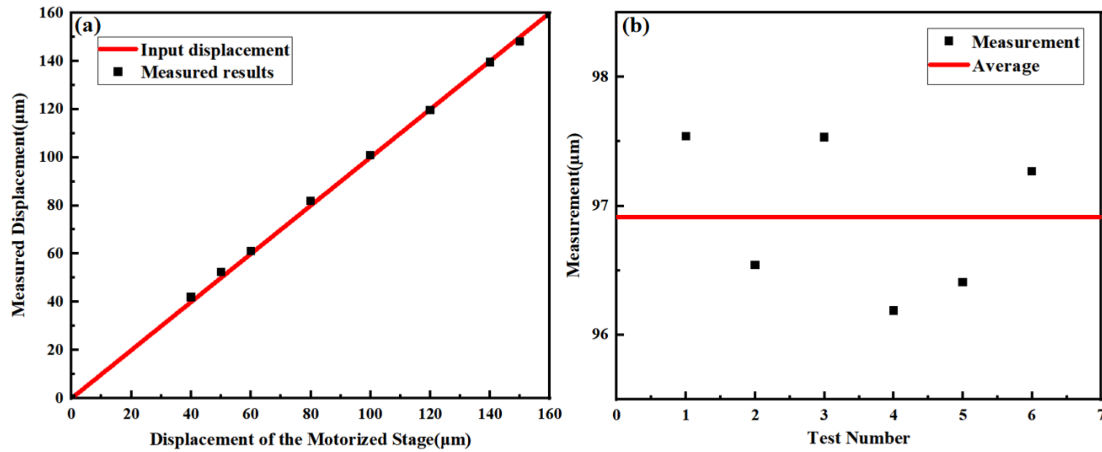

Figure 6. (a) Linear displacement measurement results obtained experimentally. The black triangle symbols indicate the results obtained from the proposed sensor. The red line indicates the input displacement. **(b)** Multiple measurement results with an input linear displacement of ~100μm. The black dots indicate the measured results. And the red line indicates the average value.

Associated with an interpolation circuits with a subdivision factor of 1000, the displacement can be measured by counting the output square signals [22]. The experimental measured results for linear displacement within a range of 160μm are shown in Figure 6(a). A motorized translation stage (MT1/M-Z8, Thorlabs) is used to provide a linear displacement. The results show well agreement between the measured results and the input displacement with a maximum error of 2.4μm, which may result from the Abbe error and the environmental vibration. Multiple measurement results shown in Figure 6(b) indicate an accuracy within ±1μm. Considering the positional repeatability of ±0.7μm for the translation stage used in the experiment, the results show a high accuracy.

According to Eq. (4), the resolution (S) of the displacement measurement can be given by [22]

$$S = \frac{d\cos\theta}{C} \tag{5}$$

where C is the subdivision factor of the interpolation circuit. As θ is small, the resolution of the linear displacement is calculated to be around 4μm/1000=4nm.

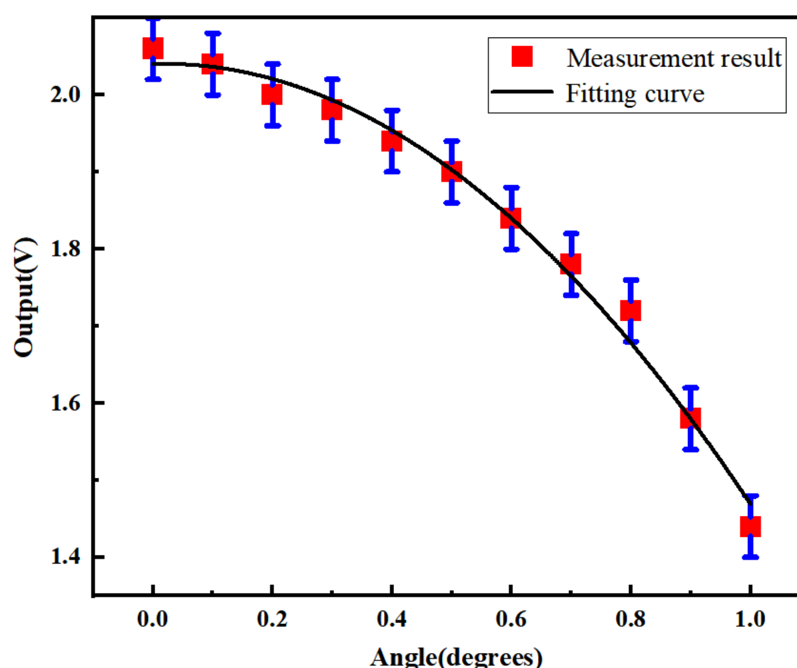

Figure 7. The relationship between the rotated angle of G1 and the amplitude of the output signal from the detector. The red dots indicate the measured results. And the black line shows the fitting curve. The error bar is mainly caused by positional error of the rotation stage.

The relationship between the rotated angle of G1 and the amplitude of the output signal from the detector is shown in Figure 7. The single-axis rotary table (RSM82-1A, Zolix) used in the experiment enables a rotation with a resolution of 2' within a range of 360°.The results show a downtrend, which agrees with the simulated results. A maximum slope of 0.92V/degree is obtained by a fitting curve with a R2 of 0.98969, resulting in a maximum sensitivity up to 0.26mV/arcsec. Considering the resolution of the voltage detecting of 1mV for the oscilloscope (TBS2204B, Tektronix) used in the experiment, a maximum total resolution of the proposed sensor for angular measurement is calculated to be ~3.85arcsec.

5. Conclusions

In this paper, we proposed a combined sensor for measuring displacement and angle synchronously based on the self-imaging effect of optical microgratings. Using a double-grating structure, the linear displacement and angle can be measured by detecting the change of the phase and amplitude of output sinusoidal signals respectively. Both the simulated and the experimental results show that, the transmitted intensity changes sinusoidally with an input linear displacement. And the amplitude of sinusoidal signals decreases with an increasing rotated angle. Associated with an interpolation circuit with a subdivision factor of 1000, linear displacement and angle measurement with a resolution of 4nm and 3.85arcsec respectively is demonstrated experimentally, which is comparable to methods such as grating diffraction interferometry and photoelectric autocollimation [29]. Since the measurement of displacement and angle is operated within one single structure, the proposed sensor shows an ultracompact structure. It is worth to mention that, benefitting from the one-single common optical path, there is no significant degradation of accuracy observed in the experiment. By using interpolation circuits with higher subdividing factor and optimizing the location of G2, a better resolution of both the linear displacement and angle measurement may be obtained. The results show the great potential of this sensor for integrated high-precision multi-DOF measurement in applications ranging from lithography machine to precision machine tools.

Preprints (www.preprints.org) | NOT PEER-REVIEWED | Posted: 27 December 2023 doi:10.20944/preprints202312.2100.v1

Author Contributions: Conceptualization, C.X. and M.Z.; methodology, C.X.; software, M.Z.; validation, H.Y. and Q.N.; formal analysis, X.Z. and J.Y.; investigation, B.J.; resources, M.L.; data curation, M.Z.; writing—original draft preparation, M.Z.; writing—review and editing, M.Z.; visualization, C.F.; supervision, C.X.; project administration, C.X. All authors have read and agreed to the published version of the manuscript.

Funding: This research was funded by National Natural Science Foundation of China (no.62375247).

Institutional Review Board Statement: Not applicable.

Informed Consent Statement: Not applicable.

Data Availability Statement: Not applicable.

Acknowledgments: The authors thank Zhiyong Yang for his helpful discussion in the experiment preparation and simulation.

Conflicts of Interest: The authors declare no conflict of interest.

References

1. Gao, W.; Kim, S. W.; Bosse, H.; Haitjema, H.; Chena, Y. L.; Lu, X. D.; Knapp, W.; Weckenmann, A.; Estler, W. T.; Kunzmann, H., Measurement technologies for precision positioning. *CIRP. Ann. Manuf. Technol.* **2015,** *64* (2), 773-796.
2. Kimura, A.; Gao, W.; Kim, W.; Hosono, K.; Shimizu, Y.; Shi, L.; Zeng, L. J., A sub-nanometric three-axis surface encoder with short-period planar gratings for stage motion measurement. *Precis. Eng.* **2012,** *36* (4), 576-585.
3. Zheng, F.; Feng, Q.; Zhang, B.; Li, J., A Method for Simultaneously Measuring 6DOF Geometric Motion Errors of Linear and Rotary Axes Using Lasers. *Sensors* **2019,** *19* (8), 1764.
4. Sun, C.; Cai, S.; Liu, Y.; Qiao, Y., Compact Laser Collimation System for Simultaneous Measurement of Five-Degree-of-Freedom Motion Errors. *Appl. Sci.* **2020,** *10* (15), 5057.
5. Chang, D.; Xing, X.; Hu, P.; Wang, J.; Tan, J., Double-Diffracted Spatially Separated Heterodyne Grating Interferometer and Analysis on its Alignment Tolerance. *Appl. Sci.* **2019,** *9* (2), 263.
6. Zhang, J.; Menq C-H., A linear/angular interferometer capable of measuring large angular mation. *Meas. Sci. Technol.* **1999,** *10* (12), 1247-1253.
7. Shimizu, S; Lee, H.-S.; Imai, N., Simultaneous measuring method of table motion errors in 6 degrees of freedom. *Int. J. Jpn. S. Prec. Eng.* **1994,** *28,* 273-274.
8. Kim, J.-A.; Kim, K.-C.; Bae, E. W.; Kim, S.; Y.K. Kwak, Six-degree-of-freedom displacement measurement system using a diffraction grating. *Rev. Sci. Instrum.* **2000,** *71* (8), 3214-3219.
9. Yin, Y.; Liu, L.; Bai, Y.; Jirigalantu; Yu, H.; Bayanheshig; Liu, Z.; Li, W., Littrow 3D measurement based on 2D grating dual-channel equal-optical path interference. *Opt. Express* **2022,** *30* (23), 41671-41684.
10. Hu, P.; Chang, D.; Tan, J.; Yang, R.; Yang, H.; Fu, H., Displacement measuring grating interferometer: a review. *Front. Inf. Technol. Electron. Eng.* **2019,** *20* (5), 631-654.
11. Lee, C. B.; Kim, G.-H.; Lee, S.-K., Uncertainty Investigation of Grating Interferometry in Six Degree-of-freedom Motion Error Measurements. *Int. J. Precis. Eng. Manuf.* **2012,** *13* (9), 1509-1515.
12. Liu, C.-H.; Cheng, C.-H., Development of a grating based multi-degree-of-freedom laser linear encoder using diffracted light. *Sens. Actuat. A-Phys.* **2012,** *181,* 87-93.
13. Hsieh, H.-L.; Pan, S.-W., Development of a grating-based interferometer for six-degree-of-freedom displacement and angle measurements. *Opt. Express* **2015,** *23* (3), 2451-2465.
14. Yu, H.; Chen, X.; Liu, C.; Cai, G.; Wang, W., A survey on the grating based optical position encoder. *Opt. Laser Technol.* **2021,** *143*.
15. Li, X.; Gao, W.; Muto, H.; Shimizu, Y.; Ito, S.; Dian, S., A six-degree-of-freedom surface encoder for precision positioning of a planar motion stage. *Precis. Eng.* **2013,** *37* (3), 771-781.
16. Wang, S.; Luo, L.; Zhu, J.; Shi, N.; Li, X., An Ultra-Precision Absolute-Type Multi-Degree-of-Freedom Grating Encoder. *Sensors* **2022**, *22* (23), 9047.
17. Yu, K.; Zhu, J.; Yuan, W.; Zhou, Q.; Xue, G.; Wu, G.; Wang, X.; Li, X., Two-channel six degrees of freedom grating-encoder for precision-positioning of sub-components in synthetic-aperture optics. *Opt. Express* **2021,** *29* (14), 21113-21128.
18. Matsukuma, H.; Ishizuka, R.; Furuta, M.; Li, X.; Shimizu, Y.; Gao, W., Reduction in Cross-Talk Errors in a Six-Degree-of-Freedom Surface Encoder. *Nanomanuf. Metrol.* **2019,** *2,* 111-123.
19. Goloborodko, A. A., Effect of random grating pit displacements on the Talbot image. *J. Opt. Soc. AM. B.* **2022,** *39* (4), 1021-1026.
20. Rodriguez-Montero, P.; Sanchez-de-La-Llave, D.; Mansurova, S., Electro-optical processor for measuring displacement employing the Talbot and the nonsteady-state photo-electromotive force effects. *Opt. Lett.* **2014,** *39* (1), 104-107.

Preprints (www.preprints.org) | NOT PEER-REVIEWED | Posted: 27 December 2023

doi:10.20944/preprints202312.2100.v1

21. Agarwal, S.; Shakher, C., In-plane displacement measurement by using circular grating Talbot interferometer. *Opt. Lasers Eng.* **2015,** *75,* 63-71.
22. Xin, C.; Yang, Z.; Qi, J.; Niu, Q.; Ma, X.; Fan, C.; Li, M., Ultra-compact displacement and vibration sensor with a sub-nanometric resolution based on Talbot effect of optical microgratings. *Opt. Express* **2022,** *30* (22), 40009-40017.
23. Liu, Q.; Ohba, R., Effects of unparallel grating planes in Talbot interferometry. *Appl. Opt.* **1999,** *38* (19), 4111-4116.
24. Wang, A.; Gill, P.; Molnar, A., Light field image sensors based on the Talbot effect. *Appl. Opt.* **2009,** *48* (31), 5897-5905.
25. Yang, Z.; Ma, X.; Yu, D.; Cao, B.; Niu, Q.; Li, M.; Xin, C., An Ultracompact Angular Displacement Sensor Based on the Talbot Effect of Optical Microgratings. *Sensors* **2023,** *23,* 1091.
26. Wronkowski, L., Diffraction model of an optoelectronic displacement measuring transducer. *Opt. Laser Technol.* **1995,** *27* (2), 81-88.
27. Zhang, Z.; Lei, B.; Zhao, G.; Ban, Y.; Da, Z.; Wang, Y.; Ye, G.; Chen, J.; Liu, H., Distance and depth modulation of Talbot imaging via specified design of the grating structure. *Opt. Express* **2022,** *30* (7), 10239-10250.
28. Teng, S.; Tan, Y.; Cheng, C., Quasi-Talbot effect of the high-density grating in near field. *J. Opt. Soc. Am. A. Opt. Image. Sci. Vis.* **2008,** *25* (12), 2945-2951.
29. Zhang, C.; Duan, F.; Fu, X.; Liu, C.; Liu, W.; Su, Y., Dual-axis optoelectronic level based on laser auto-collimation and liquid surface reflection. *Opt. Laser Technol.* **2019,** *113,* 357-364.

Disclaimer/Publisher's Note: The statements, opinions and data contained in all publications are solely those of the individual author(s) and contributor(s) and not of MDPI and/or the editor(s). MDPI and/or the editor(s) disclaim responsibility for any injury to people or property resulting from any ideas, methods, instructions or products referred to in the content.